

Radio Wave Energy Harvesting Model of a Maritime Automatic Identification System

Slunjski, Jura; Valčić, Sanjin

Source / Izvornik: **Pomorstvo**, 2023, 37, 160 - 168

Journal article, Published version

Rad u časopisu, Objavljena verzija rada (izdavačev PDF)

<https://doi.org/10.31217/p.37.1.13>

Permanent link / Trajna poveznica: <https://um.nsk.hr/um:nbn:hr:187:194605>

Rights / Prava: [In copyright](#) / [Zaštićeno autorskim pravom](#).

Download date / Datum preuzimanja: **2024-07-11**



Sveučilište u Rijeci, Pomorski fakultet
University of Rijeka, Faculty of Maritime Studies

Repository / Repozitorij:

[Repository of the University of Rijeka, Faculty of Maritime Studies - FMSRI Repository](#)





<https://doi.org/10.31217/p.37.1.13>

Radio Wave Energy Harvesting Model of a Maritime Automatic Identification System

Jura Slunjski^{1,3}, Sanjin Valčić^{1,2*}

¹ University of Rijeka, Faculty of Maritime Studies, Studentska 2, 51000 Rijeka, Croatia, e-mail: jura.slunjski@student.uniri.hr; sanjin.valcic@pfri.uniri.hr

² University of Rijeka, Faculty of Maritime Studies, Center for Marine Technologies, Milutina Barača 19, 51000 Rijeka, Croatia

³ MI MARIS d.o.o., Ulica 65. bataljuna ZNG 15, 10310 Ivanić-Grad, Croatia

* Corresponding author

ABSTRACT

Radio waves, the spectrum of the electromagnetic waves, are all around us and in most cases have only one purpose. The maritime Automatic Identification System (AIS) uses Very High Frequency (VHF) radio waves for the purpose of data exchange between ships and shore stations. These data exchanges take place during certain time intervals, resulting in intermittent emission of electromagnetic waves. In the research presented in this paper, the objective was to add a new purpose for the AIS electromagnetic waves, i.e. to act as a power source for the RF energy harvester. After collecting the electromagnetic waves of the AIS system, the signals' voltage is rectified, amplified and delivered to the load. In this paper, the process of radio wave energy harvesting is simulated in the Multisim software and analyzed in detail. The results of the analysis showed a multiple increase in the voltage value at the output of the RF energy harvester.

ARTICLE INFO

Review article

Received 11 May 2023

Accepted 28 June 2023

Key words:

Very high frequency
Automatic identification system
RF energy harvesting
Cockcroft-Walton rectifier
Impedance matching

1 Introduction

Nowadays, there is an increasing demand for cleaner and renewable energy. This means that we should strive to collect and use the energy around us, such as the energy of the radio waves, which can significantly reduce the emission of greenhouse gases, enable easier powering of wireless devices and reduce the use of batteries [1]. Namely, radio waves transfer energy and usually have only one purpose, such as establishing communications or broadcasting. Thus, there is a large number of different systems and devices that transmit radio waves at different power levels, ranging from a few milliwatts to several kilowatts, for wireless communication, i.e. for the remote reception. One such system is the maritime AIS - a communication system for navigational data exchange which uses the maritime Very High Frequency (VHF) mobile band of the radio frequency spectrum. Within this band, two channels, AIS 1 (161.975 MHz) and AIS 2 (162.025 MHz) are allocated for the standard AIS communication, and two additional channels, 75 (156.775 MHz) and 76 (156.825 MHz) for

the long-range AIS reception [2]. The data to be exchanged between devices and stations using AIS technology can be divided into static, dynamic and voyage related. This data should include the identification, position, course, speed, navigational status, etc., in order to improve navigation safety, reduce the risk of collisions and facilitate the coordination of maritime traffic. Additionally, short safety-related messages can also be exchanged between AIS devices and stations [3]. The AIS equipment can be divided into ship stations, base/shore stations, AIS Aids to Navigation (AIS AtoN), Search and Rescue (SAR) aircraft stations, AIS Search and Rescue Transmitter (AIS SART), AIS Man overboard (AIS MOB) and Emergency position indicating radio beacon AIS (EPIRB AIS).

Furthermore, ship stations can be divided into Class A, which fully complies with IMO AIS carriage requirements and the SOLAS Convention; and Class B, which is not necessarily in full accordance with IMO AIS carriage requirements and the SOLAS Convention. When these devices and stations operate in autonomous mode, the intervals of automatic data transmission vary from every 2 seconds to every

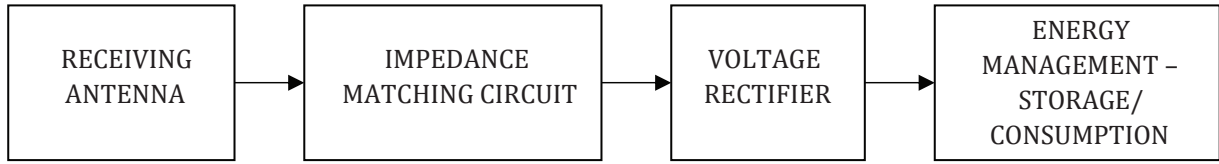


Figure 1 RF energy harvester

Source: Authors

3 minutes, depending on the type of the AIS equipment, speed and course change [4].

Considering the autonomous and continuous transmission of AIS data at different power levels, the subject of the research presented in this paper is the energy collection of AIS/VHF radio waves. In general, the energy collection process can be performed using an energy harvesting device [5]. Therefore, the primary goal of this research is to collect AIS/VHF radio waves, i.e. their energy, with the use of the RF energy harvesting device or harvester and to enable the further usage of this energy.

2 Background

The device for collecting radio waves' energy, i.e. RF energy harvester can be divided into several parts, which are shown in Figure 1 [6-10]:

- Receiving antenna,
- Impedance matching circuit;
- Voltage rectifier;
- Energy management - storage/consumption.

The receiving antenna serves as a means of collecting (receiving) radio waves and transmitting them to the guide or transmission line [11]. The performance of the receiving antenna depends on its electrical and mechanical properties, such as: antenna type, size, materials, connectors, radiation pattern, operating frequency bandwidth, impedance, gain, polarisation, voltage standing wave ratio (VSWR), etc. These and additional properties affect the total received energy, i.e. the received power of the radio waves. However, the greatest effect on the amount of the received power is the distance between the antenna of the radio wave source and the receiving antenna. If the radio waves propagate directly between those two antennas, without any obstacles, then the losses due to the spherical propagation of the radio waves can be determined according to the following expression [11]:

$$spreading\ losses = \left(\frac{\lambda}{4\pi d}\right)^2 = \left(\frac{c}{4\pi f d}\right)^2, \tag{1}$$

where λ is the radio wavelength in m, d is the distance in m, c the speed of light in m/s, f the frequency in Hz. Usually the expression (1) is stated reciprocally and in dB, and is called the Free Space Propagation Loss (FSPL):

$$\begin{aligned} FSPL(dB) &= 20 \log_{10} \frac{4\pi d}{\lambda} = 20 \log_{10} \frac{4\pi f d}{c} = \\ &= 20 \log_{10} f + 20 \log_{10} d - 147.56. \end{aligned} \tag{2}$$

In addition to the FSPL, radio wave energy losses, i.e. power losses, can occur due to the characteristics of the transmission lines or waveguides, connectors, adapters, as well as due to diffraction, refraction (fading), precipitation and atmospheric absorption, which can be difficult to assess analytically [12]. Losses can also occur due to unequal polarizations of the receiving and transmitting antennas, which depends on the angle of incidence of the radio waves on the receiving antenna [11].

After receiving the radio waves on the antenna, the signal, and thus its reduced power, must be transmitted without further reflection loss to the voltage rectifier circuit. However, the percentage of the transferred power will depend on the impedance matching of the antenna (with the transmission line) and the total impedance of the remaining circuitry (voltage rectifier and power management circuitry). In other words, when designing any RF energy harvester, it is crucial to use an impedance matching circuit, which depends on the operating frequency. Networks of coils and/or capacitors of different inductances and/or capacities are usually used to match the impedances [13-17].

The next important, if not the most important, circuit in any RF energy harvester is the voltage rectifier. Therefore, the following step is to convert the AC RF signal/voltage to the DC voltage. In most RF energy harvesting processes, the power, that is, the voltage at the input to the rectifier is very low, primarily due to FSPL. In order to solve the problem of low power at the input to the rectifier, it is possible to use a rectifier topology that also boosts up the voltage level. Such a topology would be able to extract the maximum from the electromagnetic waves' energy, and thus would increase the voltage for the consumer needs. Therefore, the entire circuitry of the RF energy harvester is faced with a choice, which is based on the consumer needs, i.e. whether the consumer requires more or less energy than is available. If the required energy is less than available, the RF energy harvester can operate continuously, while if more energy is needed, the RF energy harvester will have interruptions in operation as well as the load [7].

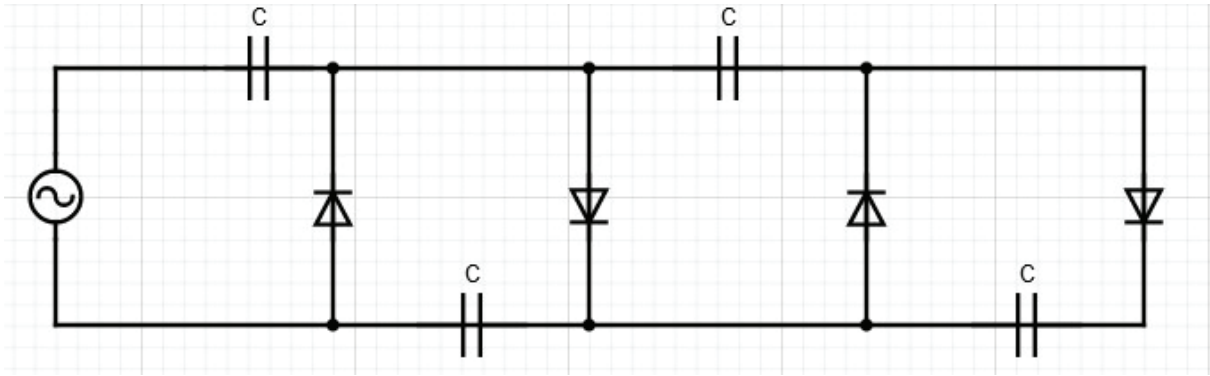


Figure 2 Two-stage Cockcroft-Walton rectifier

Source: Authors

In most of the rectifier topologies, the diodes, which exist in various designs, are most often used for voltage rectification. According to [7], some of rectifier topologies which increase the voltage are: Cockcroft-Walton, Dickson and Dickson charge pump. All the mentioned topologies at the same time rectify and amplify the voltage value at the output of the rectifier.

The Cockcroft-Walton topology operates on the principle of a half-wave rectifier, but has more levels resulting in a higher voltage amplification (Figure 2). Two diodes and two capacitors are considered one level. The operating principle of the Cockcroft-Walton rectifier is based on the charging of the capacitor, whose voltage is further added to the input voltage [18].

The Dickson rectifier topology, shown in Figure 3, is actually a modified Cockcroft-Walton rectifier that has capacitors connected in parallel to reduce the influence of parasitic effects [7].

In addition to diodes, Metal-Oxide-Semiconductor Field Effect Transistor (MOSFET) can also be used to rectify the voltage. Thus, by using MOSFET transistors, it is possible to make a modification of the Dickson rectifier, which is significantly more efficient primarily due to lower losses and greater effectiveness of the rectifier itself [7].

The last step in the RF energy harvesting process represents the energy management – storage and/or consumption of the collected radio wave energy.

3 Methodology

In this paper, the objective was to design and analyze a Multisim simulation model of the RF energy harvesting from the maritime AIS system. For this purpose, a shipborne Class B AIS transponder, whose maximum transmission power is 5 W, was considered as the AIS signal generator on the AIS 1 channel (161.975 MHz). Further-

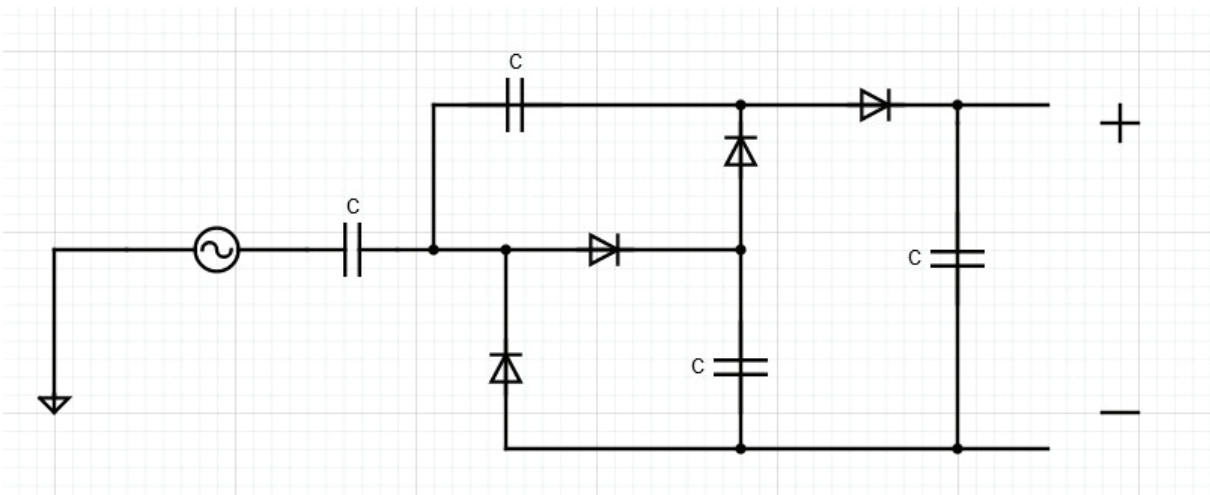


Figure 3 Two-stage Dickson rectifier

Source: Authors

more, the electrical characteristics of the transmitting, as well as the receiving antenna, were considered on the basis of a practical marine VHF antenna (Scan Antenna VHF74) [19]. This antenna is designed specifically for use in the maritime VHF mobile band, which means that it does not generate reflection losses at AIS frequencies. Moreover, its characteristic impedance is 50 Ω and the gain is 2.6 dBi.

The radio wave energy collection process was analysed at a distance of 10 m from the transmitting antenna. Such a situation can actually occur in marinas and ports, where recreational, fishing or leisure vessels can have Class B AIS transponders installed onboard. According to expression (2), the FSPL at this distance is calculated to be 36.63 dB. The power received at the receiving antenna can be determined according to the Friis transmission equation [10, 11]:

$$P_r(dBm) = P_t(dBm) + G_t(dBi) + G_r(dBi) - FSPL(dB) - L_m(dB), \tag{3}$$

where $P_r(dBm)$ is the received power in dBm, $P_t(dBm)$ is the transmitted power in dBm, $G_t(dBi)$ is the gain of the transmitting antenna in dBi, $G_r(dBi)$ is the gain of the receiving antenna in dBi and $L_m(dB)$ are the miscellaneous additional losses in dB. In this research, it was assumed that the total miscellaneous additional losses are equal to the sum of the gains of both antennas. Therefore, the received power at the receiving antenna can be determined as the difference between the transmitted power and the FSPL, which is 0.36 dBm. Given that the characteristic impedance of the antenna is 50 Ω, the RMS value of the generated voltage at the input to the voltage rectifier then amounts to 233 mV.

For the rectification purpose, a Cockroft–Walton rectifier was used in this paper, considering its practical cost-effectiveness compared to Dickson topologies. When designing Cockroft–Walton rectifiers and multipliers, the number of levels should be determined, which depends on the output characteristics. It is certainly of interest that the output voltage has as little ripple as possible, and that it is at an acceptable level for the consumer. As stated, one level consists of two capacitors and two diodes, and for the needs of the output voltage, the capacitance value of the capacitor and the number of levels which correspond to the consumer’s requirements should be determined. Several ways of determining the capacitance can be found in the literature, such as fitting all the same capacitances or reducing each capacitance starting from the first one after the power source (e.g. in the case of a 4-level rectifier, the first capacitor could theoretically have a capacitance of 8 nF, the second 7 nF, the third 6 nF and so on until the last one which would have 1 nF) [9, 21].

A Cockroft–Walton rectifier with 4 levels in a cascade topology, was modeled, simulated and analysed in this paper. For the simplification purpose, the same value of all capacitances was used. The value of the capacitance can range from 1 nF to 10 nF for the frequencies expressed in

Table 1 SPICE parameters of Schottky diode SMS7630-001

Symbol	Parameter	Units	Value
I_s	Saturation current	μA	5
R_s	Series resistance	Ω	20
N_s	Emission coefficient	-	1.05
TT	Transit time	s	1E-11
C_{j0}	Zero-bias junction capacitance	pF	0.14
M	Junction grading coefficient	-	0.4
E_G	Activation energy	eV	0.69
XTI	I_s temperature exponent	-	2
F_c	Forward bias depletion capacitance coefficient	-	0.5
B_v	Reverse breakdown voltage	V	2
I_{BV}	Reverse breakdown current	A	1E-4
V_j	Junction potential	V	0.34

Source: [20]

MHz, while in this model the capacitance of 3.3 nF is proven to be the best. This value was determined by the experimental method during the desing and testing of the simulation model. The choice of diodes plays a big role providing that the diode must have a low voltage drop and can operate at high frequencies. The voltage drop on general purpose diodes is approximately 500-700 mV and depends on the current, which extends in the range of a few mA. Also, classical diodes are not intended for the operation at high frequencies, and the main reason is their recombination time [9]. All these mentioned disadvantages of classical diodes are solved by using the Schottky diodes that have a low voltage drop and the ability to operate at high frequencies, which enables them to rectify the energy (voltage) of radio waves at frequency of 161.975 MHz.

In this model, the diode characteristics are presented using SPICE model parameters corresponding to a commercially available diode (SMS7630-001) [20]. The SPICE model parameters are actually a way of determining the parameters of components using a textual form. Therefore, in the Multisim application, in which the simulation was performed, it is possible to design diodes based on the characteristic parameters of real diodes. The SPICE model parameters are presented in Table 1.

Furthermore, in this simulation model, an arbitrarily determined parallel connection of a resistor of 100 kΩ and a capacitor of 10 nF is connected to the output of the rectifier circuit as a load.

4 Results analysis

As previously stated, the simulation model was designed in Multisim software. Due to its computational limitations, the simulation time was set to 1 ms.

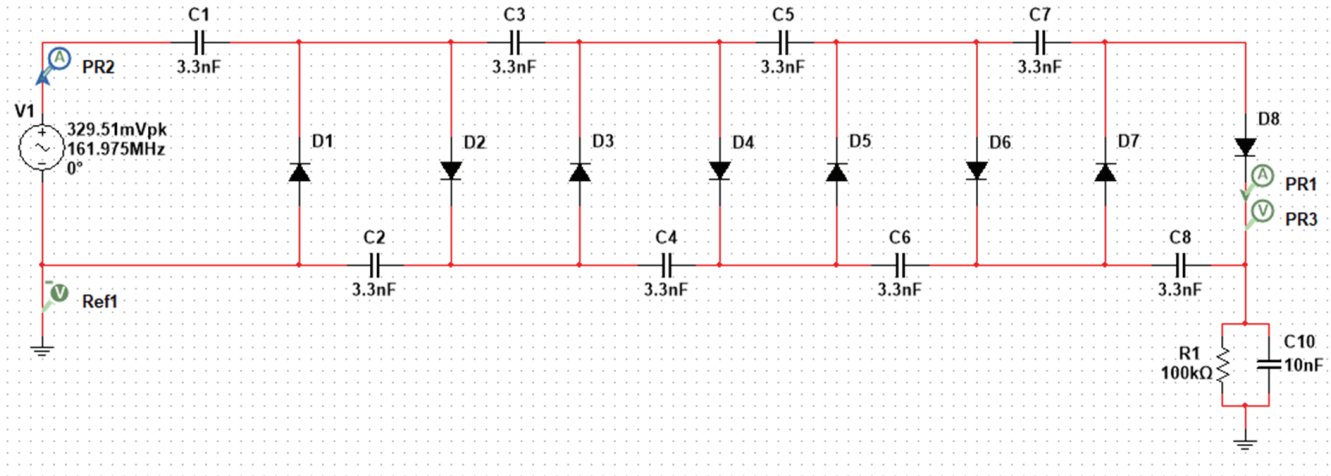


Figure 4 Multisim model of the AIS energy harvester without impedance matching

Source: Authors

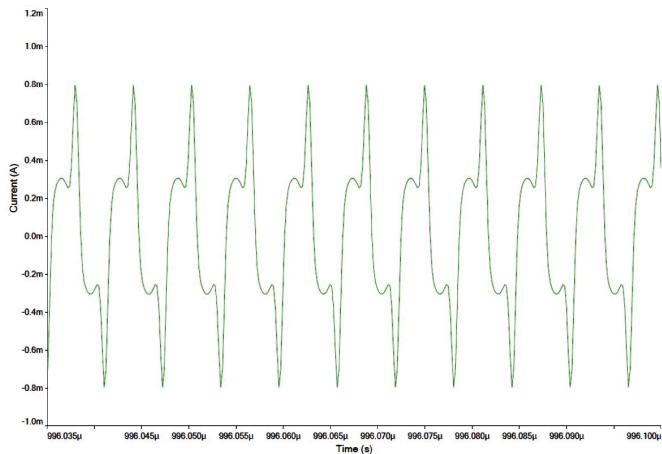


Figure 5 Input current without impedance matching

Source: Authors

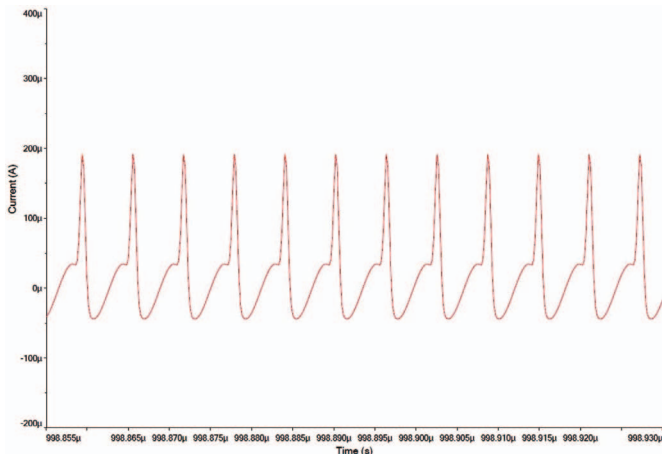


Figure 6 Output current without impedance matching

Source: Authors

First, the energy harvester model was developed without the impedance matching circuit (Figure 4). Resulting analysis is based upon the input and output current, voltage, and power, as well as on the waveform characteristics. As can be seen in Figure 4, the output current and voltage are measured after diode D8 and input current after the source V1 (characterized by the peak value of the voltage delivered by the receiving antenna).

Figures 5 and 6 show the input and the output current waveforms after the end of the simulation.

As can be seen, the input and the output current waveforms are both distorted. The main reason is that there is no impedance matching circuit, as well as the fact that the modeled energy harvester used 8 diodes that caused distortion in the input current waveform.

The RMS value of the output voltage, as well as its waveform, are shown in Figures 7 and 8.

As can be seen, after the Cockroft-Walton rectification and amplification, the output RMS voltage increased from 233 mV to 1.84 V with a peak-to-peak ripple of approximately 40 μ V.

Power measurements (Figure 9) show that the input power is 59.22 μ W, while the output power is 34.21 μ W. These power characteristics are not great, since the power efficiency of this energy harvester is 57.77%. Again, this is due to the lack of impedance matching circuitry.

Now the impedance matching circuit is implemented in two ways: 1) using parallel and series circuit resistance; and 2) with an online calculator [22].

If a simple circuit with a power source, a series resistance of the transmission line and a parallel resistance of the load, is observed, then the impedance matching is achieved using an inductor, which is connected in series, and a capacitor, which is connected in parallel. In this case, the inductor tends to affect the series resistance, while the capacitor tends to affect the parallel resistance.

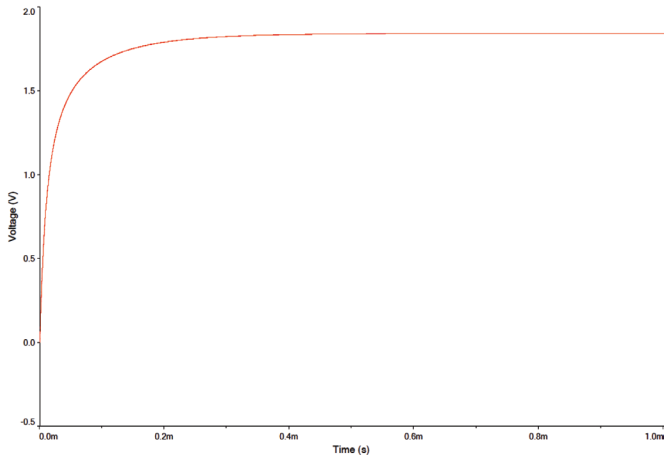


Figure 7 Output RMS voltage value without impedance matching

Source: Authors

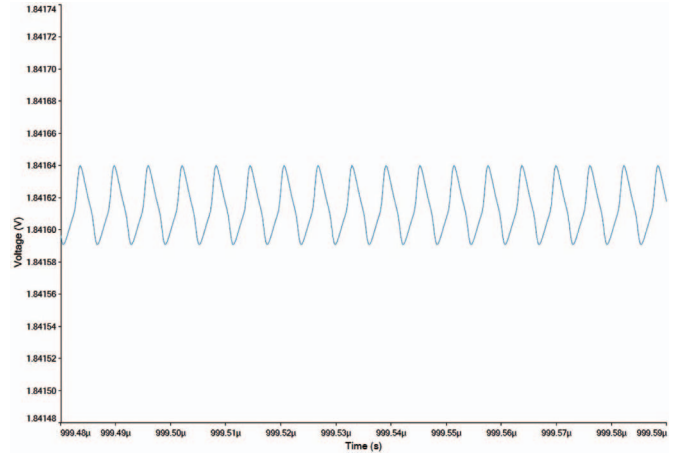


Figure 8 Output voltage waveform without impedance matching

Source: Authors

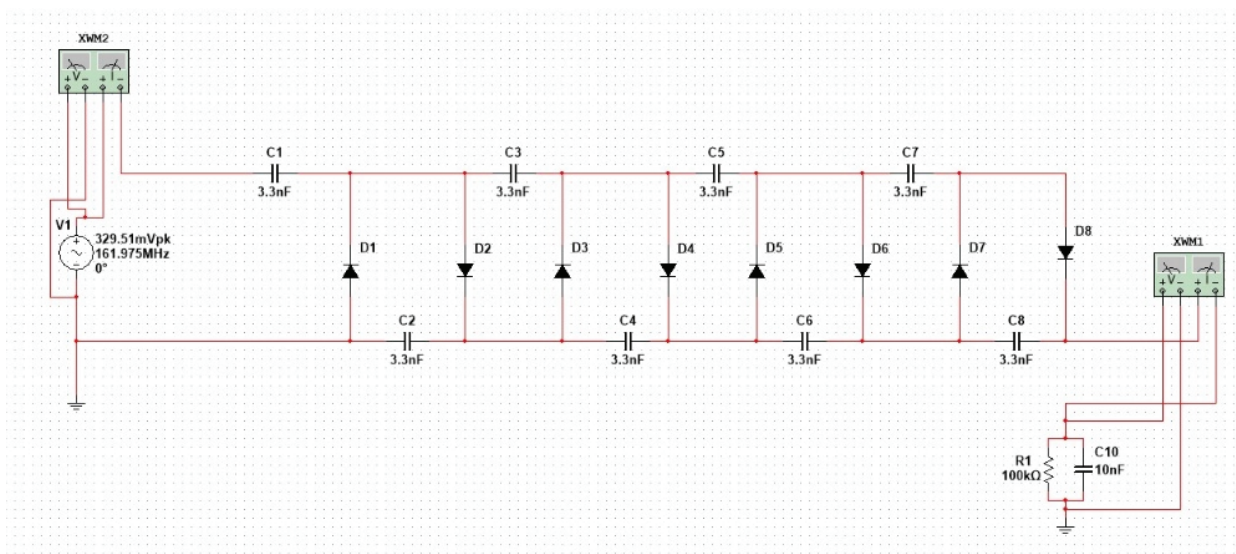


Figure 9 Power measurements without impedance matching

Source: Authors

In this model, a series (R_s) circuit resistance is based on the resistance of the transmission line (coaxial cable from the antenna) which is 50Ω , while a parallel (R_p) resistance is based on the impedance of a Cockroft-Walton rectifier with a load (Z_{in}), which can be calculated from the measured values of the input voltage and current:

$$|Z_{in}| = \left| \frac{V_{in}}{I_{in}} \right| = 520.39 \Omega \quad (4)$$

The relation between series and parallel resistance is the Q factor [23]:

$$Q = \sqrt{\frac{R_p}{R_s} - 1} = 3.07 \quad (5)$$

The reactances of the inductor (series) and the capacitor (parallel) are given by:

$$X_L = X_S = j\omega L \quad (6)$$

$$X_C = X_P = \frac{1}{j\omega C} \quad (7)$$

And series (X_s) and parallel (X_p) reactances are:

$$X_S = Q \cdot R_S \quad (8)$$

$$X_P = \frac{R_P}{Q} \quad (9)$$

Finally, the values of the inductance and the capacitance required for the impedance matching are:

$$L = \frac{X_S}{\omega} = 150.83 \text{ nH} \tag{10}$$

$$C = \frac{1}{\omega X_P} = 5.68 \text{ pF} \tag{11}$$

By implementing the inductor and the capacitor after the voltage source in the model previously shown in Figure 4, the analysis of currents, voltages and powers follows.

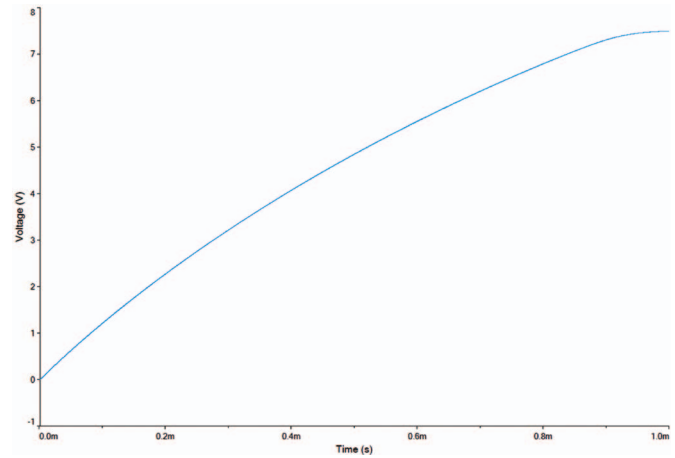


Figure 12 Output RMS voltage value with series and parallel resistance impedance matching

Source: Authors

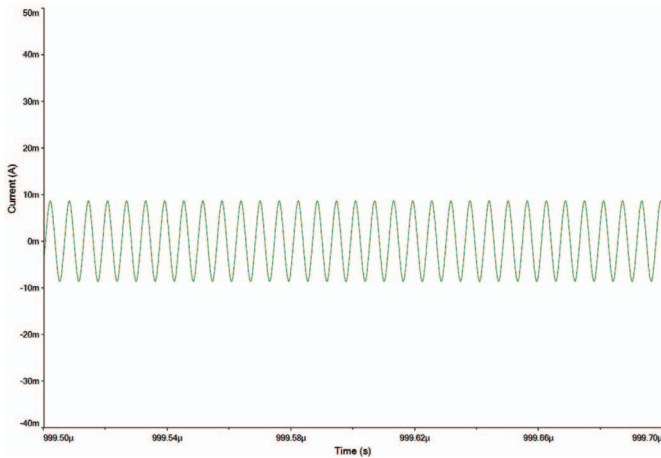


Figure 10 Input current with series and parallel resistance impedance matching

Source: Authors

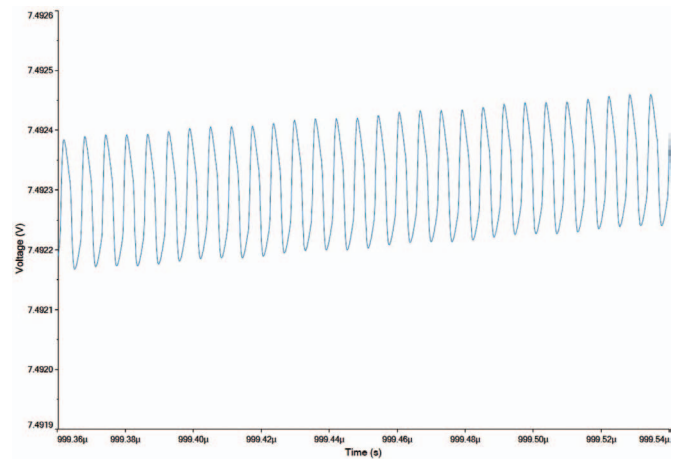


Figure 13 Output voltage waveform with series and parallel resistance impedance matching

Source: Authors

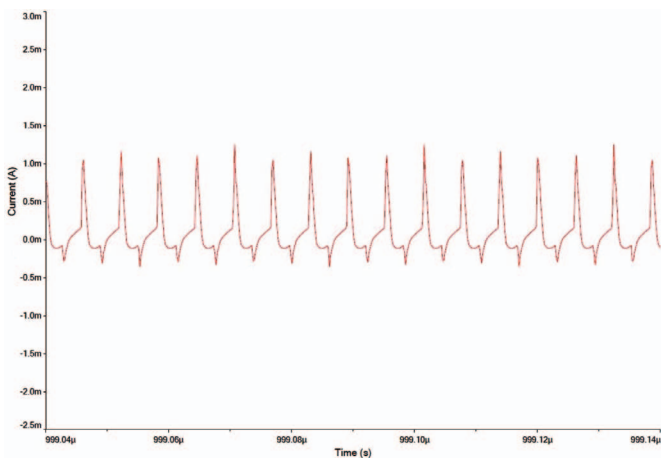


Figure 11 Output current with series and parallel resistance impedance matching

Source: Authors

As can be seen in Figures 10-13, both input and output waveforms are improved but still not ideal. Input power in this case equals to 1.19 mW, while the output power is 601.54 µW. Increased output power confirms the efficiency of the impedance matching circuit. However, the power efficiency in this case is only 50.55%.

The impedance matching using an online calculator [22], gives the capacitor value of 4.11 pF and the inductor value of 170 nH. Inserting those values into the simulation model, resulting current waveforms are shown in Figures 14 and 15.

The output voltage is shown in Figures 16 and 17.

After using the online impedance matching calculator, the input power is reduced to 1.07 mW, while the output

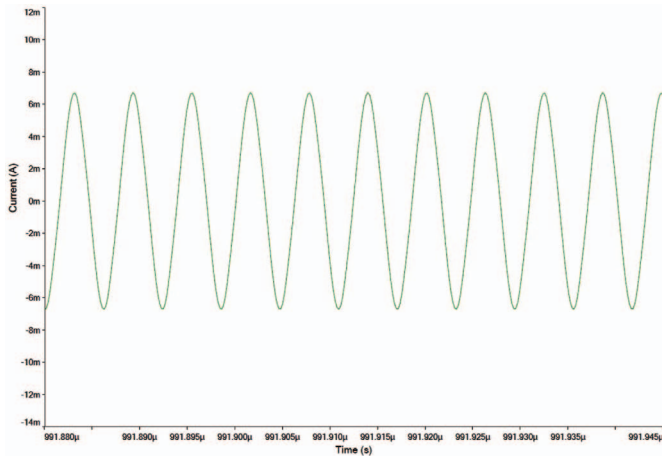


Figure 14 Input current with online impedance matching calculator

Source: Authors

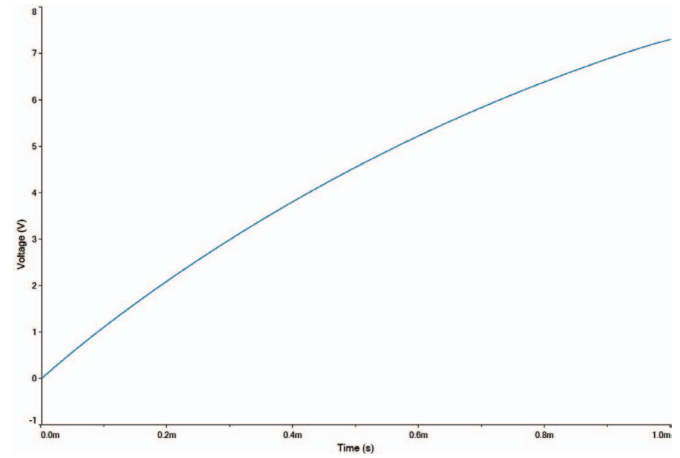


Figure 16 Output RMS voltage value with online impedance matching calculator

Source: Authors

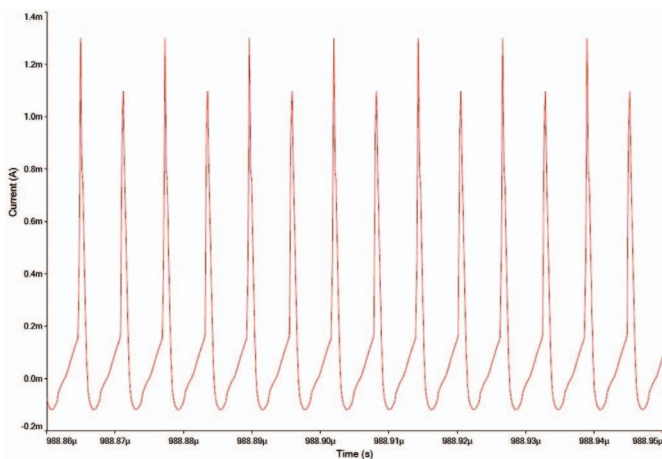


Figure 15 Output current with online impedance matching calculator

Source: Authors

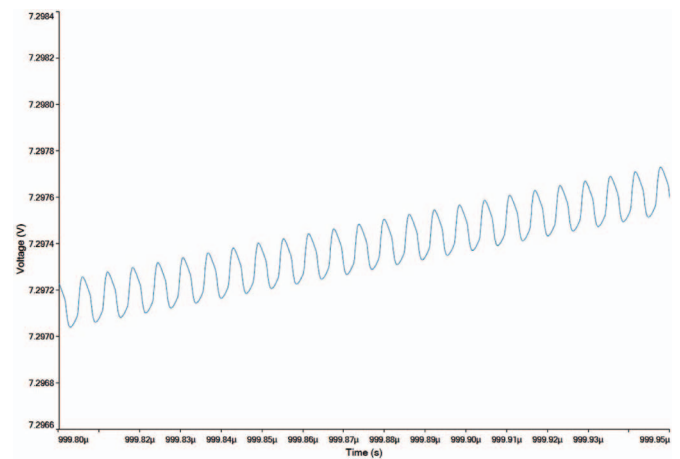


Figure 17 Output voltage waveform with online impedance matching calculator

Source: Authors

power equals to 798.42 μ W. In addition, the power efficiency equals to 74.62% which indicates that most of the power has been transferred from the source to the load with this type of the impedance matching.

As can be seen from the previous analysis, in both cases when the impedance matching circuit was used, the RMS value of the output voltage was above 7 V. Furthermore, it can be observed that the output voltage kept increasing during the simulation time, when the impedance matching circuit was used (Figures 12 and 16).

On the other hand, in case when the impedance matching circuit was not used, after approximately 0.3 ms, the output voltage remained at a constant value (Figure 7).

5 Conclusion

In this paper, a Multisim simulation model of the AIS energy harvester based on the Cockroft-Walton voltage rectifier and multiplier was developed and analysed. The analyzed parameters included input and output characteristics of the current, voltage and power. The input power and voltage were based on AIS signal transmission at a distance of 10 m, with a power of 5 W. It was calculated that the voltage at the input to the Cockroft-Walton rectifier and multiplier was 233 mV.

After running the simulations, the results have been significantly improved after implementing the impedance matching circuit. In other words, after adding the impedance matching circuit, the output voltage increased by ap-

proximately 7 V in comparison to the input voltage. In addition, the power factor also increased on both the input and the output side and there were also less distortions in input and output waveforms.

Therefore, this analysis showed that it is necessary to balance both sides – the input and output of the energy harvester, and even the rectifier, for the most efficient energy transfer from the antenna to the load.

Although only simulation results were presented in the paper, the energy harvesting of the electromagnetic waves generated by the Automatic Identification System can be used in various ways, which could ultimately be proven by conducting a practical experiment with the proper RF energy harvester device.

The analysis carried out in this research also opens the possibilities for further testing and performing simulations using the Cockcroft–Walton rectifiers with different capacity values, as well as using the other rectifier topologies which also increase the voltage level.

Funding: The research presented in the manuscript did not receive any external funding.

Author Contributions: Both authors contributed to the manuscript equally.

References

- [1] Pozo, B., Garate, J.I., Araujo, J.Á.; Ferreira, S. Energy Harvesting Technologies and Equivalent Electronic Structural Models—Review. *Electronics* 2019, 8, 486. <https://doi.org/10.3390/electronics8050486>.
- [2] International Telecommunication Union, Recommendation ITU-R M.1371-5: Technical characteristics for an automatic identification system using time division multiple access in the VHF maritime mobile frequency band, *Electronic Publication*, Geneva, 2014.
- [3] International Maritime Organization, Recommendation on Performance Standards for an Universal Shipborne Automatic Identification System (AIS), Resolution MSC 74(69), Annex 3, 1998.
- [4] International Maritime Organization, Revised Guidelines for the Onboard Operational Use of Shipborne Automatic Identification System (AIS), Resolution A.1106(29), 2015.
- [5] Adamu, M., Ang, L.-M., Prabaharan, S. & Seng, K.P., Radio frequency energy harvesting and management for wireless sensor networks, Book Chapter, *Green Mobile Devices and Networks*, 1st Edition, CRC Press, Boca Raton, Florida, USA, 2012.
- [6] Pareja Aparicio, M. et al., Radio Frequency Energy Harvesting – Sources and Techniques, Book Chapter, *Renewable Energy – Utilisation and System Integration*, IntechOpen, London, UK, 2016.
- [7] Tran, L.G., Cha, H.K. & Park, W.T. RF power harvesting: a review on designing methodologies and applications. *Micro and Nano Syst Lett* 5, 14 (2017). <https://doi.org/10.1186/s40486-017-0051-0>.
- [8] Bougas, I.D., Papadopoulou, M.S., Boursianis, A.D., Kokkinidis, K., Goudos, S.K. State-of-the-Art Techniques in RF Energy Harvesting Circuits. *Telecom* 2021, 2, 369–389. <https://doi.org/10.3390/telecom2040022>.
- [9] Langdon, T., Very Low Power Cockcroft-Walton Voltage Multiplier for RF Energy Harvesting Applications. *Electrical Engineering Undergraduate Honors Theses*, 2019, Retrieved from <https://scholarworks.uark.edu/eleguht/69>.
- [10] Ibrahim, H.H., Singh, M.J., Al-Bawri, S.S., Ibrahim, S.K., Islam, M.T., Alzamil, A., Islam, M.S., Radio Frequency Energy Harvesting Technologies: A Comprehensive Review on Designing, Methodologies, and Potential Applications. *Sensors* 2022, 22, 4144. <https://doi.org/10.3390/s22114144>.
- [11] Balanis, Constantine A. *Antenna Theory: Analysis and Design*. 3rd ed. John Wiley, 2005.
- [12] Richards, J.A., *Radio Wave Propagation: An Introduction for the Non-Specialist*, Springer-Verlag Berlin, Heidelberg, Germany, 2008, <https://doi.org/10.1007/978-3-540-77125-8>.
- [13] Penella, M.T., Gasulla, M., *Powering Autonomous Sensors - An Integral Approach with Focus on Solar and RF Energy Harvesting*, Springer Netherlands, Springer Science + Business Media, 2011, doi:10.1007/978-94-007-1573-8.
- [14] Le, T.T., *Efficient Power Conversion Interface Circuits for Energy Harvesting Applications*, PhD Thesis, Oregon State University, 2008.
- [15] Curty, J.P., Joehl, N., Krummeanacher, F., Dehollain, C., Declercq, M.J., A model for u-Power Rectifier Analysis and Design, *IEEE Transactions on Circuits and systems I*, 2005.
- [16] Muramatsu, M., Koizumi, H., An Experimental Result using RF Energy Harvesting Circuit with Dickson Charge Pump, *IEEE Conference on Sustainable Energy Technologies (ICSET)*, Sri Lanka, 2010.
- [17] Olgun, U., Chen, C.C., Volakis, J.L., Investigation of Rectenna Array Configurations for Enhanced RF Power Harvesting, *IEEE Antennas and Wireless Propagation Letters*, Vol. 10, pp. 262-265, 2011.
- [18] Patel, A.P, Rathod, M., Design, Simulation and Construction of Cockroft Walton Voltage Multiplier, *GRD Journal for Engineering*, Volume 1, Issue 4, *Global Research and Development Journals*, India, 2016.
- [19] Scan-Antenna, VHF74, Technical specifications, Available on <https://www.scan-antenna.com/products/vhf74>, Accessed on 17 May 2023.
- [20] Skyworks Solutions, Inc., SMS7630-001 Datasheet, 2005, Available on: <https://www.rf-microwave.com/en/skyworks/sms7630-001/zero-bias-schottky-diode/sms7630-001/>, Accessed on 17 May 2023.
- [21] Xiang, Z., Han, S., Liu, B., Peng, H., Wang Z. & Sun, G., Design and Analysis of a PMOS RF-DC Conversion Circuit at UHF for Ambient Energy Harvesting, 2019 IEEE/CIC International Conference on Communications Workshops in China (ICCC Workshops), Changchun, China, 2019, pp. 59-64, doi: 10.1109/ICCCChinaW.2019.8849957.
- [22] Analog Devices, Inc., RF Impedance Matching Calculator, <https://www.analog.com/en/design-center/interactive-design-tools/rf-impedance-matching-calculator.html>, Accessed on 17 May 2023.
- [23] Bramble, S., Radio Frequency (RF) Impedance Matching: Calculations and Simulations, Technical Article, 2021, Analog Devices, Inc.